Detecting archaic introgression without archaic reference genomes

Laurits Skov[1*], Ruoyun Hui[2], Asger Hobolth[1], Aylwyn Scally[2], Mikkel Heide Schierup[1], Richard Durbin[2*]

1. Bioinformatics Research Centre, Aarhus University, 8000 Aarhus C., Denmark
2. Department of Genetics, University of Cambridge, Cambridge CB2 3EH United Kingdom

*Correspondence: lskov@cs.au.dk, rd@sanger.ac.uk

Abstract

Human populations out of Africa have experienced at least two bouts of introgression from archaic humans, Neandertal and Denisovans. In Papuans there is prior evidence of both these introgressions. Here we present a new approach to detect segments of individual genomes of archaic origin without using an archaic reference genome. The approach is based on the detection of genomic regions with a high SNV density of SNVs not seen in unadmixed populations. We show using simulations that this provides a powerful approach to identifying segments of archaic introgression with a small rate of false detection. Furthermore our approach is able to accurately infer admixture proportions and divergence time of human and archaic populations.

We apply the model to detect archaic introgression in 89 Papuans and show how the identified segments can be assigned to likely Neandertal or Denisovan origin. We report more Denisovan admixture than previous studies and directly find a shift in size distribution of fragments of Neandertal and Denisovan origin that is compatible with a difference in admixture time. Furthermore we identify small amounts of Denisova ancestry in West Eurasians, South East Asians and South Asians.

Introduction

Archaic introgression into modern humans occurred at least twice (Neandertals and Denisovans) (MEYER *et al.* 2012; PRUFER *et al.* 2014) and had a phenotypic effect on humans (HUERTA-SANCHEZ *et al.* 2014; DANNEMANN *et al.* 2017; RACIMO *et al.* 2017). A large part of Neandertal and Denisovan genetic material is still present in modern humans and we can learn about archaic populations from studying the effect of their genetic variants in humans.

To harness this information a number of methods have been developed to infer segments of archaic ancestry in an individual's genome.

Scanning along the genome, Hidden Markov Models (HMMs)(PRUFER *et al.* 2014; SEGUIN-ORLANDO *et al.* 2014) and Conditional Random Fields (CRF)(SANKARARAMAN *et al.* 2016) can identify haplotypes in non-Africans that are 1. closer to the archaic reference genomes, than to Africans and 2. are longer than expected by incomplete lineage sorting, and these are then identified as archaic introgressed segments. Another approach is to identify segments with more variants in higher linkage disequilibrium (LD) that are unique to non-Africans than expected given a certain demographic scenario (PLAGNOL and WALL 2006). The latest implementations of this method also use an archaic reference genome for refining the set of putative archaic haplotypes (VERNOT *et al.* 2016).

The use of archaic reference genomes for identification of introgressed fragments has drawbacks. First, since the Neandertal reference genomes are closer to the introgressing Neandertal (80,000-145,000 years divergence)(PRUFER *et al.* 2017) , than the introgressing Denisova is to the Denisova genome (276,000-403,000 years divergence)(PRUFER *et al.* 2014) detecting Denisovan ancestry will be harder. Second, the reliance on having reference genomes implies that the introgression maps generated by these methods need updates whenever more archaic reference genomes are sequenced (PRUFER *et al.* 2017). Finally, it may be hard to identify introgressing segments of unknown archaic origin if such exists, as in the case of the putative archaic introgression into Pygmies (HSIEH *et al.* 2016) and Andamanese islanders (MONDAL *et al.* 2016).

Here we present a new method for the identification of archaic introgression that does not require a reference genome or prior knowledge of demographic parameters, but uses density of variants

in individuals private to their population of origin. We demonstrate with Papuans how we can estimate demographic parameters relevant to introgression and infer more archaic material than previously. Furthermore, we can separate introgression events into Denisovan and Neandertal components that display different length distributions in accordance with different admixture times.

Method

Model

An archaic genomic segment introgressed into a population is expected to have a high density of variants not found in populations without the introgression. We use a Hidden Markov Model (HMM) to classify genomic segments into states with varying variant density. We focus on a scenario where introgression with a deeply divergent archaic population only happened into an ingroup and not the outgroup, see Figure 1, panel a.

We can then remove variants found in the outgroup in order to better distinguish the variant density in introgressed segments and non-introgressed segments, see Figure 1, panel a. These remaining variants which we denote private variants (because they are private with respect to the ingroup) can either have occurred on the branch starting from the split of the ingroup and outgroup or if they are introgressed, they could have occurred on the introgressing population's branch. Because the introgressing segments have had a longer time to accumulate variants, they have a higher probability of emitting private variants.

Thus, we define a HMM with two states. The hidden states are Ingroup and Archaic, and the probability for changing state in the Ingroup is *p* and the probability for changing state in the Archaic is *q*, see Figure 1, panel b. The probability of changing state can also be expressed in terms of a constant recombination rate between windows $r \cdot L$, the admixture time T_{admix} and admixture proportion a, Figure 1, panel b. We show how to derive it in Supplementary note 1.

The number of private variants observed in a window of length *L* (typically $L = 1000\ bp$) is Poisson distributed with a rate $\lambda_{Ingroup}$ and $\lambda_{Archaic}$, respectively where $\lambda_{Ingroup} = \mu \cdot L \cdot T_{Ingroup}$ and $\lambda_{Archaic} = \mu \cdot L \cdot T_{Archaic}$. μ is the mutation rate, $T_{ingroup}$ is the mean coalescence time for the ingroup and the outgroup and $T_{Archaic}$ is the mean coalescence time for the archaic population and the outgroup, see Figure 1, panel c.

88 We make a correction of the rates to take into account the number of missing bases in a window
89 and the local mutation rate. For window i we have $\lambda^i_{Ingroup} = \mu_i \cdot L_i \cdot T_{Ingroup}$ and $\lambda^i_{Archaic} = \mu_i \cdot$
90 $L_i \cdot T_{Archaic}$, where μ_i is the local mutation rate and L_i is the number of called bases in a widow.

91 The set of transition parameters p, q and the Poisson parameters $\lambda_{Ingroup}$, $\lambda_{archaic}$ that
92 maximizes the likelihood given the observations are found using the Baum-Welch algorithm for an
93 individual genome. These parameters are informative of the mean coalescence with the ingroup
94 and archaic with the outgroup, the admixture time and the admixture proportion if we assume a
95 known mutation rate μ and a known recombination rate between windows rL.

96 Once the set of optimal parameters are found they can be used to decode the genome, using
97 posterior decoding. We call each window where the posterior probability of being in the archaic
98 state is bigger than 0.5 as archaic. We group consecutive archaic windows together into archaic
99 segments and calculate the mean posterior probability of being archaic for the entire segment.

100

101 **Results**

102 *Testing the model with simulations*

103 To investigate the ability of our model to identify archaic (Neandertal and Denisovan) admixture
104 into Papuans we simulated un-phased whole autosome data with admixture with an archaic
105 hominin 1,500 generations ago replacing 5% of the population – (a script with all demographic
106 parameters are shown in Supporting information – Simulation script.py and a graphic
107 representation of the demography is shown in Supporting figure 1). We simulated three scenarios
108 to test the effects of missing data and varying recombination rate. The mutation rate were kept
109 constant across the genome for all simulations.

110 First, we simulated five individuals where every base in the genome is called equally well and
111 there is a constant recombination rate of $1.2 \cdot 10^{-8}$ events per basepair per generation. We call
112 this dataset the ideal data. Second, we simulated five individuals and removed all variants that are
113 in repetitive regions (using the repeatmask track for the human reference genome hg19 (SMIT *et*
114 *al.* 2013)) to test how the model performs with missing data. Third, we simulated five individuals
115 with missing data and using a varying recombination rate (using HapMap phase II (INTERNATIONAL

116 HAPMAP *et al.* 2007)) to test the effect of missing data and recombination. We analyzed all
117 genomes in bins of 1000 bp, and removed all variants found in 500 simulated Africans, 100
118 simulated Europeans and 100 simulated Asians. We combine two haplotypes to form genotype
119 data for the simulated individuals. This will be more similar to situations where phased data is not
120 available. For diploid data the conversion from p, q, $\lambda_{Ingroup}$ and $\lambda_{Archaic}$ to $T_{archaic}$, $T_{Ingroup}$,
121 T_{admix} and a changes as is shown in Supplementary note 1.

122 We found the transition and emission parameters that optimized the likelihood, using the Baum-
123 Welch algorithm and used them to get an estimate for the admixture time T_{admix}, the admixture
124 proportion a and the mean coalescent times with the outgroup $T_{ingroup}$ and $T_{archaic}$ for the
125 ingroup and archaic segments respectively, see Figure 2 panel b.

126 For all scenarios the coalescence time between the ingroup and outgroup ($T_{ingroup}$) the mean
127 estimate is 2,625 generations ago(max = 2,647, min = 2,595), and the average simulated
128 coalescent time with the outgroup is 3,109 generations ago. For the coalescence time between
129 the outgroup and the archaic ($T_{archaic}$) the mean estimate is 37,345 generations ago (max =
130 37,832, min = 37,028) and the simulated values were 35,543 generations ago.

131 We find that the mean estimate of the admixture proportion a when using the transition matrix is
132 between 4.62 % and 5.34 %.

133 We also find that with a posterior cutoff at 0.8 for segments (mean posterior probability of being
134 archaic for all windows in segment), the amount of false positives can be reduced to around 50%,
135 while still keeping 90% of the true segments, see Supporting figure 4.

136 An estimate of the false negative rate of the model is counting the amount of simulated archaic
137 segments that have zero overlap with the putative archaic sequence, which is 11.1 Mb for ideal
138 simulations, 32.2 Mb for simulations with missing data and 26.3 Mb for simulations with missing
139 data and a varying recombination rate, see Figure 2 panel a. The model has less power to identify
140 short segments as can be seen in Supporting figure 2.

141 If we estimate the false positive rate as the amount of putative archaic segments that have zero
142 overlap with the simulated archaic segments we find 8.4 Mb for ideal simulations, 4.1 Mb for
143 simulations with missing data and 9.0 Mb for simulations with missing data and a varying

144 recombination rate, see Figure 2 panel a. In total, we recover 243 Mb, 198 Mb and 184 Mb of
145 archaic sequence for Ideal simulations, simulations with missing data and simulations with missing
146 data and varying recombination rate respectively.

147 An example of how the simulated and putative archaic segments overlap is shown in Figure 2,
148 panel c for the a 10 Mb window. A map of all simulated archaic segments and putative archaic
149 segments can be seen in Supporting figure 3.

150 The mean estimate for the admixture time using transition matrix is around 1,704 generations ago
151 when using the ideal data and 1,522 generations ago when adding missing data. When we vary the
152 recombination rate across the genome the average estimate of the admixture time is 1,146
153 generations ago if we estimate it using the transition matrix. The underestimate of the admixture
154 time might be due to fact that the model fail to identify around 80% of the short segments. This
155 would make the average segment length longer and make the admixture time seem more recent.

156

157 *Application to Papuan genomes*

158 Having verified the validity of the model, we applied it to 14 Papuan individuals from Simons
159 diversity project (MALLICK *et al.* 2016), 40 Papuans from (MALASPINAS *et al.* 2016) and an additional
160 35 Papuans (VERNOT *et al.* 2016). In addition to this, we also analyzed individuals from West
161 Eurasia, East Asia and South East Asia.

162 For each individual we used two different sets of variants as outgroup. We estimate the
163 background mutation rate in windows of 100 kb, using the variant density of all variants in the
164 African populations from the 1000 genomes project.

165 Our model will not be able to distinguish Neandertal from Denisova segments in Papuans, because
166 the Denisovans and Neandertals share a common ancestor before they do with humans and
167 therefore the mean coalescence time with humans will be the same (PRUFER *et al.* 2014). This
168 means that the Poisson parameters will be the same as they both depend on $T_{archaic}$. However,
169 we should be able to enrich for Denisova and Neandertal segments by using different outgroups in
170 our filtering step.

171 First, we used only variants found in Sub-Saharan populations as an outgroup. This should remove
172 variation in the common ancestor of Sub-Saharan Africans and the Papuans, retaining archaic
173 variants of Neandertal and Denisova origin as both are present in Papuans, but mainly absent in
174 Africa (SANKARARAMAN *et al.* 2016; VERNOT *et al.* 2016). We also used this filter when analyzing
175 Eurasian populations.

176 Second we remove variants found in all non Papuan populations, only retaining variants that are
177 unique to Papuan populations. This should remove Neandertal variants that are shared with other
178 non-African populations (PRUFER *et al.* 2014) and also to some extend remove variants of Denisova
179 origin that are mainly found in Asians and Native Americans (SKOGLUND and JAKOBSSON 2011; QIN
180 and STONEKING 2015). Thus removing all variants from 1000 genomes should enrich for Denisova
181 segments while the segments that do not overlap when using the two different outgroups should
182 be enriched for Neandertal segments.

183 We found the optimal set of transition and emission parameters for each Papuan individual and
184 found them to be largely consistent across the different datasets, See Supporting figure 5. The
185 parameters were converted into estimates of T_{admix}, a, $T_{ingroup}$ and $T_{archaic}$ using an average
186 recombination rate of and mutation rate of $1.2 \cdot 10^{-8}$ events per basepair per generation and an
187 average mutation rate of $1.25 \cdot 10^{-8}$ mutations per base pair per generation, see Figure 3, panel a
188 and b.

189 We find that mean coalescence time between Papuans and non-Papuan individuals happened
190 more recently (1,395 – 1,540 generations ago) than the mean coalescence time with Sub-Saharan
191 Africans (1,953-2,293 generations ago) reflecting that Papuans are more closely related to other
192 Non-Africans than to Africans. The mean coalescence time between Papuans and other non-
193 Africans also provides an upper limit for Neandertal introgression because it happened into the
194 common ancestor of these populations.

195 Using only Sub-Saharan individuals as an outgroup we find a mean coalescence time to between
196 the archaic and outgroup to be between 29,404 and 33,944 generations ago. When using non-
197 Papuans as an outgroup the estimate is between 25,268 and 30,352 generations ago. The lower
198 estimate is likely due to the fact that some of the variants in the common ancestor of Denisovans
199 and Neandertals have been removed.

200 We estimate the admixture proportion of archaic sequence to between 4.1-4.4 % and the
201 admixture proportion that is unique to Papuans between 1.5-1.8 %. This means that around 2.6 %
202 is shared with Non-Papuans, see Figure 3, panel a.

203 Using the transition parameters we estimate that both admixture events happened around 1000
204 generations ago which is likely an underestimate as it was for the simulated data with missing data
205 and varying recombination rate. Neandertal admixture likely occurred some 2,000 generations ago
206 after the out of Africa migration (FU *et al.* 2014; SANKARARAMAN *et al.* 2016) and Denisova admixture
207 likely occurred before the peopling of Sahul which is thought to be 47-55 thousand years ago
208 (1,620-1,896 generations ago assuming a generation time of 29 years) (CLARKSON *et al.* 2015;
209 O'CONNELL and ALLEN 2015), if one assumes that Denisova ancestry in Asians, Native Americans and
210 Papuans have the same origin.

211 We use a threshold of 0.8 posterior probability as in the case of the simulated data. By comparing
212 to the Vindija (PRUFER *et al.* 2017) and Denisova (MEYER *et al.* 2012) genomes we find that this
213 cutoff removes around 50% of the short segments that don't share variants with any archaic
214 reference genome and could be deeply coalescing modern human haplotypes, see Supporting
215 figure 8.

216 When we use a cutoff of 0.8 we find that 84 % of the segments unique to Papuans (80 % of the
217 total sequence) shared more variants Denisova genome than Vindija and that 78 % the segments
218 that are shared with other non-Africans (83 % of the total sequence) shared more variants with
219 the Vindija Neandertal than the Denisova, See Figure 3, panel c. This means that a majority of the
220 archaic sequence unique to Papuans likely comes from a population more closely related to
221 Denisovans.

222 However, segments that are unique to Papuans are longer on average (94.2 kb) compared to
223 those shared with other non-African populations (76.9 kb), See Figure 3, panel d. The difference in
224 length distributions are not seen as clearly when using Sstar or CRF, see Supporting figure 6.
225 Moreover, the length distribution of archaic segments that are not unique to Papuans are more
226 similar to other non-African populations, see Supporting figure 7.

227 We compared our archaic segments to those previously reported using other methods
228 (SANKARARAMAN *et al.* 2016; VERNOT *et al.* 2016). We find that 67% of the archaic sequence found

229 using CRF are also recovered using our method, and that 74% of the archaic sequence found using
230 Sstar are also recovered using our method.

231 Comparing to the archaic reference genomes our method finds more Denisova in Papuans than it
232 finds Neandertal unlike the CRF. It also finds a significant amount of additional Denisova segments
233 in East and South East Asians, see Table 1.

234

Model	*Pop*	*Both*	*Denisova*	*None*	*Vindija*	*Total*
HMM	Papuan	4.40	77.00	11.39	71.44	164.23
	eastasia	1.48	5.69	9.96	61.37	78.49
	southasia	1.62	5.85	10.12	51.36	68.95
	westeurasia	1.47	2.39	10.14	43.95	57.94
Sstar	Papuan	26.5	43.11		49.21	118.82
	eastasia	-	0.00	-	65.02	65.02
	southasia	-	0.00	-	55.18	55.18
	westeurasia	-	0.00	-	51.23	51.23
CRF	Papuan	-	58.17	-	84.72	142.89
	eastasia	-	3.21	-	72.92	76.14
	southasia	-	2.79	-	61.36	64.15
	westeurasia	-	0.68	-	57.29	57.97

235

236 **Table 1. Amount of sequence of different origins.** The amount of sequence (in Mb) that is equally
237 related to Denisova and Vindija, more closely related to Denisova, doesn't share any variation with
238 either and is more closely related to Vindija are shown different populations and different
239 methods.

240

241

242 **Discussion**

243 Since emission probabilities are very different between the human and archaic states in our
244 model, we expect a low rate of false positive archaic inference and this is also what we see in
245 simulations made to match the real data closely. However, since recombination rates are highly
246 variable, a lot of very short archaic segments are expected and these have a very high false
247 negative rate. Our inability to identify these cause us to underestimate of the admixture time.
248 However the model does seem to find the correct size distribution for longer segments (> 50 kb),
249 see Supporting figure 2. The mean coalescence times of modern and archaic humans is estimated
250 well in simulations. In real data, the potential presence of super-archaic introgression as reported
251 into the sequenced Denisovan (PRUFER *et al.* 2014) should cause us to overestimate this quantity,
252 but this effect is expected to be small since there is little difference between Europeans and
253 Papuans for this quantity. It remains to be seen whether there is also evidence for super-archaic
254 admixture in the introgressing Denisova. One way to do this would be to just add an extra super-
255 archaic hidden state to our model.

256

257 Our model reports more Denisova segments than approaches relying on the Denisovan reference.
258 This is likely because our method does not rely on putative Denisova segments being more closely
259 related to the Denisova genome than the Vindija Neandertal genome. Given that the introgressing
260 and sequenced Denisova split shortly after the Neandertals split from Denisovans (PRUFER *et al.*
261 2014) many segments are expected to be equally close to the Vindija Neandertal and Denisova. It
262 is also expected that a fraction of segments introgressed for Denisova are more closely related to
263 Vindija and vice verse due to incomplete lineage sorting. It is therefore also reassuring that we do
264 not find the same large excess of Neanderthal fragments in Papuans compared to Asian
265 populations as has been reported previously, see Table 1.

266

267 We find no clear evidence for an introgression with a new archaic hominin in Papuans, but we do
268 find segments that do not share variation with any of the sequenced archaic populations. These
269 segments could likely represent variation in Neandertals and Denisovans that is not captured by
270 the three high coverage archaic reference genomes. In the future it will be interesting to compare

271 these segments to other human populations that might also have archaic segments of unknown
272 origin (HSIEH *et al.* 2016; MONDAL *et al.* 2016).
273
274 Our model works particularly well when it is possible to remove all the common variation between
275 the ingroup and outgroup. As a larger number of individuals from different species are being
276 sequenced, this method could be used as an alternative method for identifying introgression in
277 other species, e.g. chimp bonobo (DE MANUEL *et al.* 2016), bears (LIU *et al.* 2014), elephants
278 (PALKOPOULOU *et al.* 2018) or gibbons (CARBONE *et al.* 2014).
279

280 **Materials and methods**

281 **Simulations**

282 To simulate data we used Msprime (KELLEHER *et al.* 2016). We simulated 5 Papuans and as an
283 outgroup we simulated 500 Africans, 100 Europeans and 100 Asians using demographic
284 parameters from (MALASPINAS *et al.* 2016). We simulated data where we varied the recombination
285 rate according to HapMap recombination maps (INTERNATIONAL HAPMAP *et al.* 2007) for 5 individuals
286 and removed variants within non-callable regions and variants that were found in the simulated
287 outgroup. We grouped all autosomes into bins of 1000 base pairs and counted the number of
288 variants. For each 1000 bp windows we calculated the number of called bases using the repeat
289 masked segments.

290

291 **Train parameters and decode segments**

292 We trained and decoded the segments using our HMM, which is available at:
293 https://github.com/LauritsSkov/Introgression-detection/

294

295 **Data sets**

296 We used 14 Papuans, 71 WestEurasians, 72 East Asians and 39 South Asians individuals from
297 Simons diversity project (MALLICK *et al.* 2016), 40 Papuans form (MALASPINAS *et al.* 2016) and an
298 additional 35 Papuans (VERNOT *et al.* 2016).

299

300 **Filtering variants in real data**

301 We used two sets of outgroups. One is all Sub-Saharan Africans (populations: YRI, MSL, ESN) from
302 1000 Genomes Project (GENOMES PROJECT *et al.* 2015) and all Sub-Saharan African populations from
303 Simons (MALLICK *et al.* 2016) (not Masai, Somali, Sharawi and Mozabite).
304 The other ougroup is all individuals from the 1000 Genomes (GENOMES PROJECT *et al.* 2015) as
305 outgroup and all Non-Papuans from Simons diversity project.
306 For all human data sets, we also removed sites that fell within repeatmasked (SMIT *et al.* 2013)
307 regions, and sites that were not in the Strict callability mask for the 1000 genomes Project.
308 Repeat mask regions
309 hgdownload.cse.ucsc.edu/goldenpath/hg19/bigZips/chromFaMasked.tar.gz

310

311 Strict callability mask for 1000 genomes:

312 ftp://ftp.1000genomes.ebi.ac.uk/vol1/ftp/release/20130502/supporting/accessible_genome_mas

313 ks/StrictMask/

314

315 The background mutation rate was calculated using the variants density of all variants from

316 populations YRI, LWK, GWD, MSL and ESN in windows of 100 Kb divided by the mean variant

317 density of the whole genome.

318

319 **Comparison to Sstar and Conditional Random Field**

320 We called Neandertal and Denisova segments in the 14 Papuans and compared them to the

321 segments called with CRF with more than 50 posterior probability (SANKARARAMAN *et al.* 2016)

322 available at:

323 **https://sriramlab.cass.idre.ucla.edu/public/sankararaman.curbio.2016/**

324 The path to the haplotypes is:

325 summaries/2/denisova/oceania/summaries/haplotypes/CRHOM.thresh-50.length-0.00.haplotypes

326

327 We called Neandertal and Denisova segments in the 35 Papuans and compared them to the

328 segments called with Sstar with more than 99 posterior probability (VERNOT *et al.* 2016) available

329 at:

330 https://drive.google.com/drive/folders/0B9Pc7_zItMCVWUp6bWtXc2xJVkk

331 The path to the haplotypes is:

332 introgressed_haplotypes/LL.callsetPNG.mr_0.99.den_calls_by_hap.bed.merged.by_chr.bed

333

334 **Calculation of admixture time using length distribution**

335 We fitted a linear regression line to the log of the length distribution of putative archaic segments

336 with a posterior probability greater than 0.5. The slope is an estimate of the mean of the

337 exponential distribution and can be converted into an admixture time using

338 $mean\ of\ exponential = \frac{1}{(1-m)r(t-1)}$ where where m is the admixture proportion, t is the

339 admixture time and r is the recombination rate per base pair.

340 **Figure legends**

341 **Figure 1. Overview of the model.** Illustration on small test dataset. a) An archaic segment
342 introgresses into the ingroup population at time T_{admix} with admixture proportion a. The
343 segments in the ingroup has a mean coalescence time with a segment from the outgroup at time
344 $T_{Ingroup}$ and an archaic segment has a mean coalescence time with a segment from the outgroup
345 at time $T_{Archaic}$. Removing all variants found in the outgroup (light orange points) should remove
346 all the variants in the common ancestor of ingroup and outgroup, leaving only private variants that
347 either occurred on the ingroup branch (dark orange) or on the archaic branch (dark blue). This will
348 make the archaic segment have a higher variant density. The genome is then binned into windows
349 of *L* (here 1000 bp) and the number of private variants are counted in each window. These are the
350 observations and the hidden states are either Ingroup state or Archaic state. When decoding the
351 sequence the most likely path through the sequence is found. b) The transition matrix between
352 the archaic state and ingroup state. c) The emission probabilities are modelled as Poisson
353 distributions with means $\lambda_{Ingroup}$ and $\lambda_{Archaic}$. It is more likely to see more private variants in the
354 Archaic state than in the Ingroup state.

355

356 **Figure 2. Evaluation of the model on simulated data.** a) Average amount of sequence per
357 individual that come from segments that are classified as false archaic (zero percent overlap with
358 any true archaic segment), found < 50% (segment where there is less than 50 % overlap with true
359 archaic segments), found > 50 % (segments where more than 50 % overlap with true archaic
360 segments) and missed archaic which are segments that the model does not identify as archaic. The
361 bars are colored according to what simulation scenarios they belong to. All segments are used
362 here are required to have > 0.8 posterior probability. b) The estimation of the four parameters
363 T_{admix}, a, $T_{ingroup}$ and $T_{archaic}$ are shown for the different simulation scenarios. c) And example
364 of how simulated archaic segments and putative archaic segments overlap in a 10 Mb window.
365 The x-axis is the genomic coordinates in Mb and the y-axis is the different simulation scenarios.

366

367 **Figure 3. Application of model to Papuan genomes.** a) Relationship between modern and archaic
368 humans with the outgroup branches (Sub-Saharan Africans) colored in red. The average
369 coalescence times for ingroup and outgroup $T_{Ingroup}$ and archaic and outgroup $T_{Archaic}$ are
370 shown. The admixture proportions a and admixture time T_{admix} are shown for segments that are
371 shared with other non-African populations. b) The outgroup colored in red is now all non-Papuans,
372 and the new demographic parameters are shown. c) The segments that are shared with other
373 Non-Africans share more variation with the Vindija Neandertal than they do with the Altai
374 Denisova. Segments that are unique to Papuan individuals share more variation with Altai
375 Denisova than they do with the Vindija Neandertal. d) The length distribution (all archaic segments
376 with a mean posterior probability > 0.5 are kept) for segments that are shared with other non-
377 African populations is shorter than segments that are unique to Papuans.

378

379 **Supporting Figure legends**

380 **Supporting figure 1 – Demographic parameters for simulation.** The effective population sizes,
381 split times and bottleneck population sizes are shown for the simulated populations.

382 **Supporting figure 2 - Total segments and sequence called SIM.** The first column show the total
383 number of segments found and the second column show the total amount of sequence that these
384 segments add up to. The rows are different simulation scenarios and the colors of the stacked bar
385 plot show the amount/number of segments that are not found using posterior decoding, where
386 less than half of the segment overlap with the true archaic segments or where more than half of
387 the segment overlaps with the true archaic segment.

388 **Supporting figure 3- True and inferred archaic for the whole genome for simulated data.** The x-
389 axis is the genomic coordinates and the y-axis is the simulated individual. We colored the
390 segments according to if they are true archaic of inferred archaic by the model using a cutoff of 0.5
391 for the mean posterior probability of the segment.

392 **Supporting figure 4 – Effect of adjusting cutoff for when to include a putative archaic segment.**
393 The rows are different simulation scenarios and the rows are different classifications of putative
394 archaic segments. False is segments with zero overlap to the true archaic segments, found<50%

395 are archaic segments that overlap with less than 50% with the true archaic segments and
396 found>50% are segments that overlap with more than 50% with the true archaic segments. On
397 the x-axis is the mean posterior probability of an archaic segment and the y-axis is the amount of
398 sequence left when applying the filter.

399

400 **Supporting figure 5 - Parameter estimation of Papuans.** The different facets show the estimates
401 for the parameters t_admix, a, T_ingroup and T_archaic depending on which outgroup was used
402 (Sub-Saharan Africans or the whole world (non-Papuans). The bars are colored according to which
403 dataset they came from.

404 **Supporting figure 6 - Length distribution other methods.** The length distribution of all Denisova
405 and Neandertal segments found using conditional random field (CRF), the hidden Markov model
406 (HMM) and Sstar. For the HMM Neandertal are those segments that are shared with other non-
407 African populations and Denisova are those unique to Papuans.

408

409 **Supporting figure 7 - Length distribution of Asia, Europe and Papuans.** The length distribution of
410 segments unique to Papuans (Denisova) and segments shared with other non-African populations
411 (Neandertal) are shown for four different population groups.

412

413 **Supporting figure 8 - Closeness to archaic humans with cutoff.** The probability of a segment
414 sharing any variants with the archaic reference genomes as a function of the average posterior
415 probability of a segment.

416 **References**

417 Carbone, L., R. A. Harris, S. Gnerre, K. R. Veeramah, B. Lorente-Galdos *et al.*, 2014 Gibbon genome
418 and the fast karyotype evolution of small apes. Nature 513: 195-201.
419 Clarkson, C., M. Smith, B. Marwick, R. Fullagar, L. A. Wallis *et al.*, 2015 The archaeology,
420 chronology and stratigraphy of Madjedbebe (Malakunanja II): A site in northern Australia
421 with early occupation. J Hum Evol 83: 46-64.
422 Dannemann, M., K. Prufer and J. Kelso, 2017 Functional implications of Neandertal introgression in
423 modern humans. Genome Biol 18: 61.
424 de Manuel, M., M. Kuhlwilm, P. Frandsen, V. C. Sousa, T. Desai *et al.*, 2016 Chimpanzee genomic
425 diversity reveals ancient admixture with bonobos. Science 354: 477-481.
426 Fu, Q., H. Li, P. Moorjani, F. Jay, S. M. Slepchenko *et al.*, 2014 Genome sequence of a 45,000-year-
427 old modern human from western Siberia. Nature 514: 445-449.
428 Genomes Project, C., A. Auton, L. D. Brooks, R. M. Durbin, E. P. Garrison *et al.*, 2015 A global
429 reference for human genetic variation. Nature 526: 68-74.
430 Hsieh, P., A. E. Woerner, J. D. Wall, J. Lachance, S. A. Tishkoff *et al.*, 2016 Model-based analyses of
431 whole-genome data reveal a complex evolutionary history involving archaic introgression
432 in Central African Pygmies. Genome Res 26: 291-300.
433 Huerta-Sanchez, E., X. Jin, Asan, Z. Bianba, B. M. Peter *et al.*, 2014 Altitude adaptation in Tibetans
434 caused by introgression of Denisovan-like DNA. Nature 512: 194-197.
435 International HapMap, C., K. A. Frazer, D. G. Ballinger, D. R. Cox, D. A. Hinds *et al.*, 2007 A second
436 generation human haplotype map of over 3.1 million SNPs. Nature 449: 851-861.
437 Kelleher, J., A. M. Etheridge and G. McVean, 2016 Efficient Coalescent Simulation and Genealogical
438 Analysis for Large Sample Sizes. PLoS Comput Biol 12: e1004842.
439 Liu, S. P., E. D. Lorenzen, M. Fumagalli, B. Li, K. Harris *et al.*, 2014 Population Genomics Reveal
440 Recent Speciation and Rapid Evolutionary Adaptation in Polar Bears. Cell 157: 785-794.
441 Malaspinas, A. S., M. C. Westaway, C. Muller, V. C. Sousa, O. Lao *et al.*, 2016 A genomic history of
442 Aboriginal Australia. Nature 538: 207-214.
443 Mallick, S., H. Li, M. Lipson, I. Mathieson, M. Gymrek *et al.*, 2016 The Simons Genome Diversity
444 Project: 300 genomes from 142 diverse populations. Nature 538: 201-206.
445 Meyer, M., M. Kircher, M. T. Gansauge, H. Li, F. Racimo *et al.*, 2012 A high-coverage genome
446 sequence from an archaic Denisovan individual. Science 338: 222-226.
447 Mondal, M., F. Casals, T. Xu, G. M. Dall'Olio, M. Pybus *et al.*, 2016 Genomic analysis of
448 Andamanese provides insights into ancient human migration into Asia and adaptation. Nat
449 Genet 48: 1066-1070.
450 O'Connell, J. F., and J. Allen, 2015 The process, biotic impact, and global implications of the human
451 colonization of Sahul about 47,000 years ago. Journal of Archaeological Science 56: 73-84.
452 Palkopoulou, E., M. Lipson, S. Mallick, S. Nielsen, N. Rohland *et al.*, 2018 A comprehensive genomic
453 history of extinct and living elephants. Proc Natl Acad Sci U S A 115: E2566-E2574.
454 Plagnol, V., and J. D. Wall, 2006 Possible ancestral structure in human populations. PLoS Genet 2:
455 e105.
456 Prufer, K., C. de Filippo, S. Grote, F. Mafessoni, P. Korlevic *et al.*, 2017 A high-coverage Neandertal
457 genome from Vindija Cave in Croatia. Science.
458 Prufer, K., F. Racimo, N. Patterson, F. Jay, S. Sankararaman *et al.*, 2014 The complete genome
459 sequence of a Neanderthal from the Altai Mountains. Nature 505: 43-49.

460 Qin, P., and M. Stoneking, 2015 Denisovan Ancestry in East Eurasian and Native American
461 Populations. Mol Biol Evol 32: 2665-2674.
462 Racimo, F., D. Gokhman, M. Fumagalli, A. Ko, T. Hansen *et al.*, 2017 Archaic Adaptive Introgression
463 in TBX15/WARS2. Mol Biol Evol 34: 509-524.
464 Sankararaman, S., S. Mallick, N. Patterson and D. Reich, 2016 The Combined Landscape of
465 Denisovan and Neanderthal Ancestry in Present-Day Humans. Curr Biol 26: 1241-1247.
466 Seguin-Orlando, A., T. S. Korneliussen, M. Sikora, A. S. Malaspinas, A. Manica *et al.*, 2014
467 Paleogenomics. Genomic structure in Europeans dating back at least 36,200 years. Science
468 346: 1113-1118.
469 Skoglund, P., and M. Jakobsson, 2011 Archaic human ancestry in East Asia. Proc Natl Acad Sci U S A
470 108: 18301-18306.
471 Smit, A. F. A., R. Hubley and P. Green, 2013 RepeatMasker Open 4.0. RepeatMasker Open 4.0.
472 Vernot, B., S. Tucci, J. Kelso, J. G. Schraiber, A. B. Wolf *et al.*, 2016 Excavating Neandertal and
473 Denisovan DNA from the genomes of Melanesian individuals. Science 352: 235-239.
474

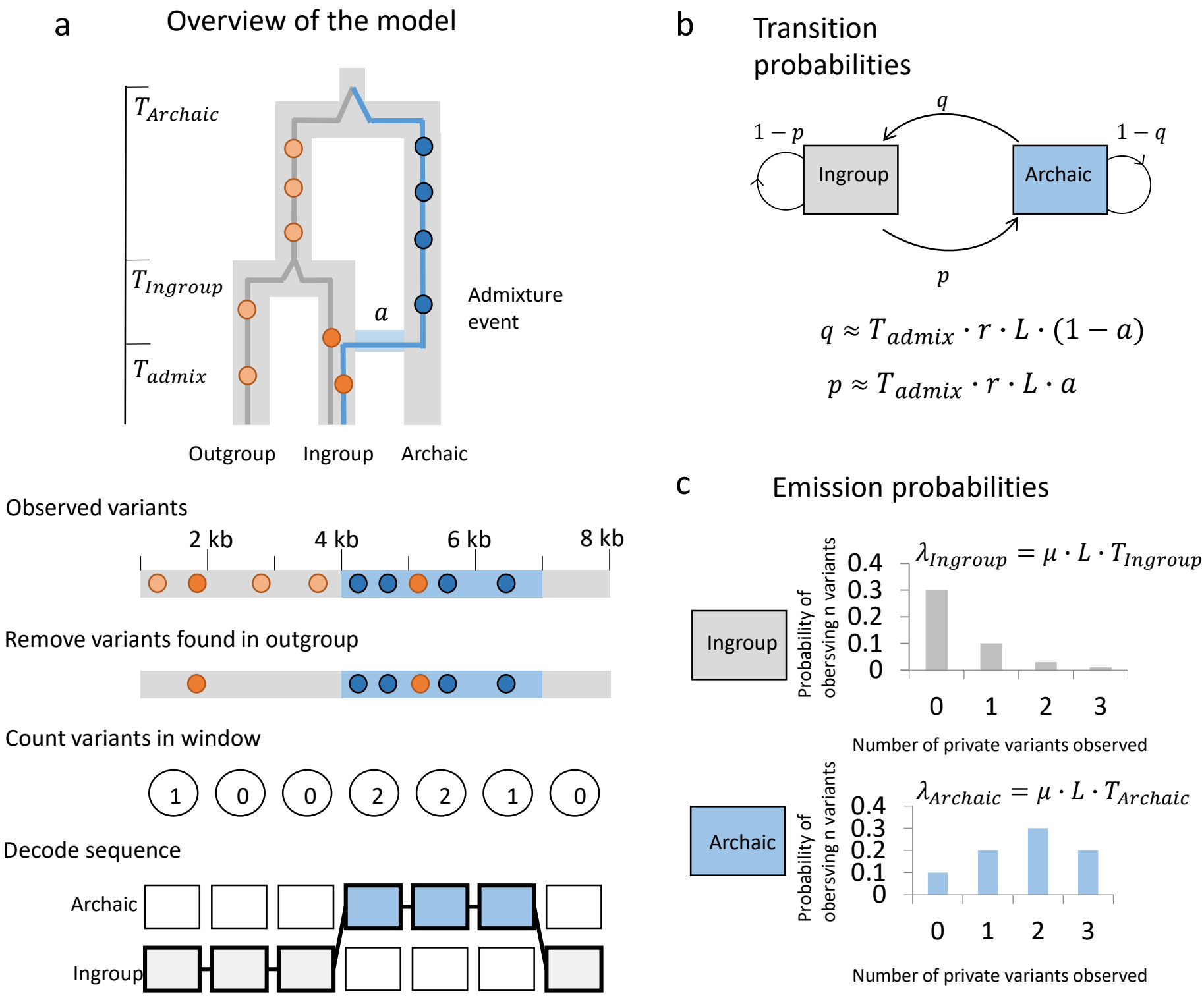
a
Overview of the model
$T_{Archaic}$
$T_{Ingroup}$
T_{admix}
a
Admixture event
Outgroup
Ingroup
Archaic
Observed variants
2 kb
4 kb
6 kb
8 kb
Remove variants found in outgroup
Count variants in window
1 0 0 2 2 1 0
Decode sequence
Archaic
Ingroup
b
Transition probabilities
q
$1-p$
$1-q$
Ingroup
Archaic
p
$q \approx T_{admix} \cdot r \cdot L \cdot (1-a)$
$p \approx T_{admix} \cdot r \cdot L \cdot a$
c
Emission probabilities
Ingroup
$\lambda_{Ingroup} = \mu \cdot L \cdot T_{Ingroup}$
Probability of obersving n variants
0.4
0.3
0.2
0.1
0
0 1 2 3
Number of private variants observed
Archaic
$\lambda_{Archaic} = \mu \cdot L \cdot T_{Archaic}$
Probability of obersving n variants
0.4
0.3
0.2
0.1
0
0 1 2 3
Number of private variants observed

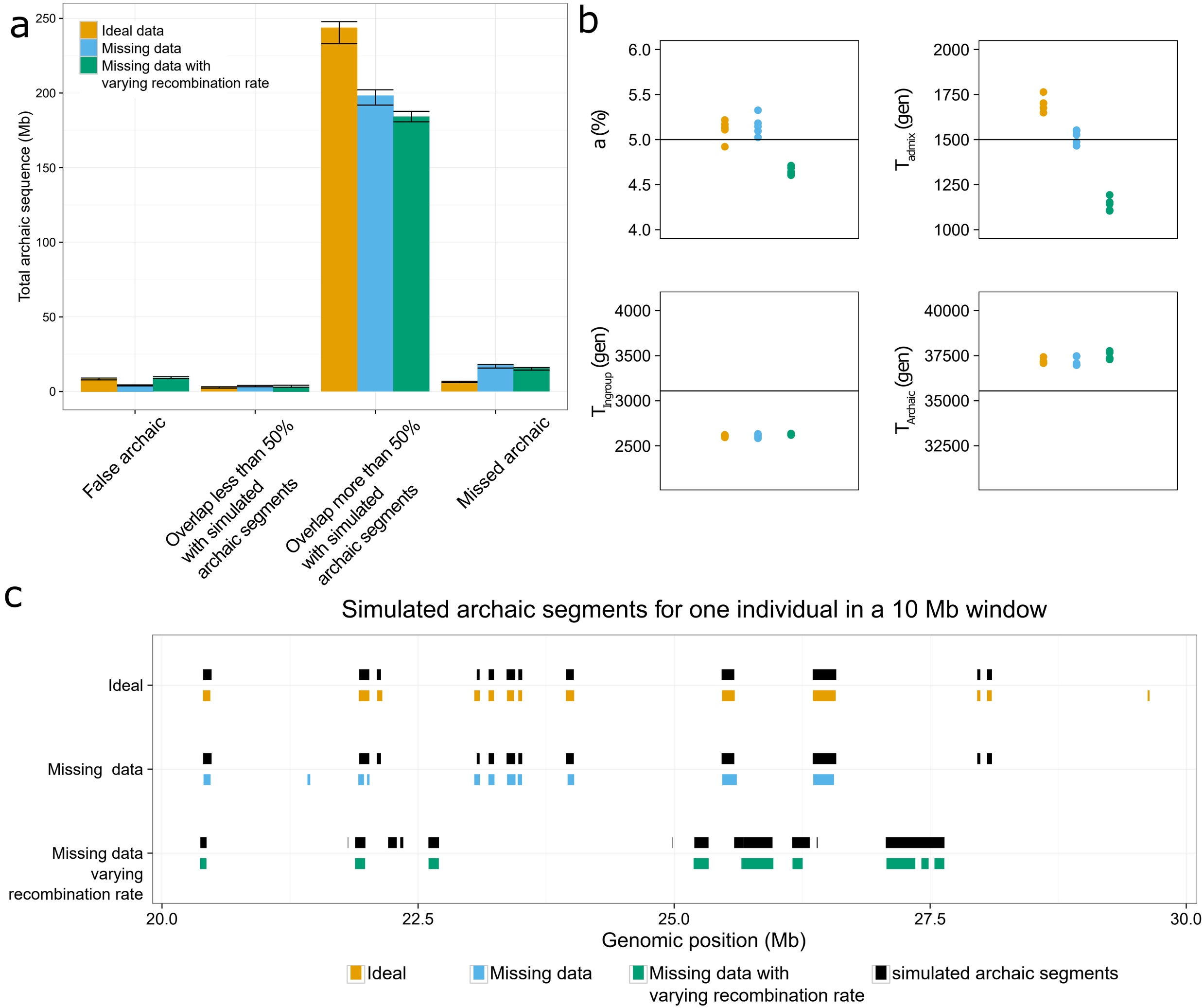
a
Ideal data
Missing data
Missing data with
varying recombination rate
Total archaic sequence (Mb)
250
200
150
100
50
0
False archaic
Overlap less than 50%
with simulated
archaic segments
Overlap more than 50%
with simulated
archaic segments
Missed archaic
b
a (%)
6.0
5.5
5.0
4.5
4.0
T_{admix} (gen)
2000
1750
1500
1250
1000
$T_{Ingroup}$ (gen)
4000
3500
3000
2500
$T_{Archaic}$ (gen)
40000
37500
35000
32500
c
Simulated archaic segments for one individual in a 10 Mb window
Ideal
Missing data
Missing data
varying
recombination rate
20.0
22.5
25.0
27.5
30.0
Genomic position (Mb)
Ideal
Missing data
Missing data with
varying recombination rate
simulated archaic segments

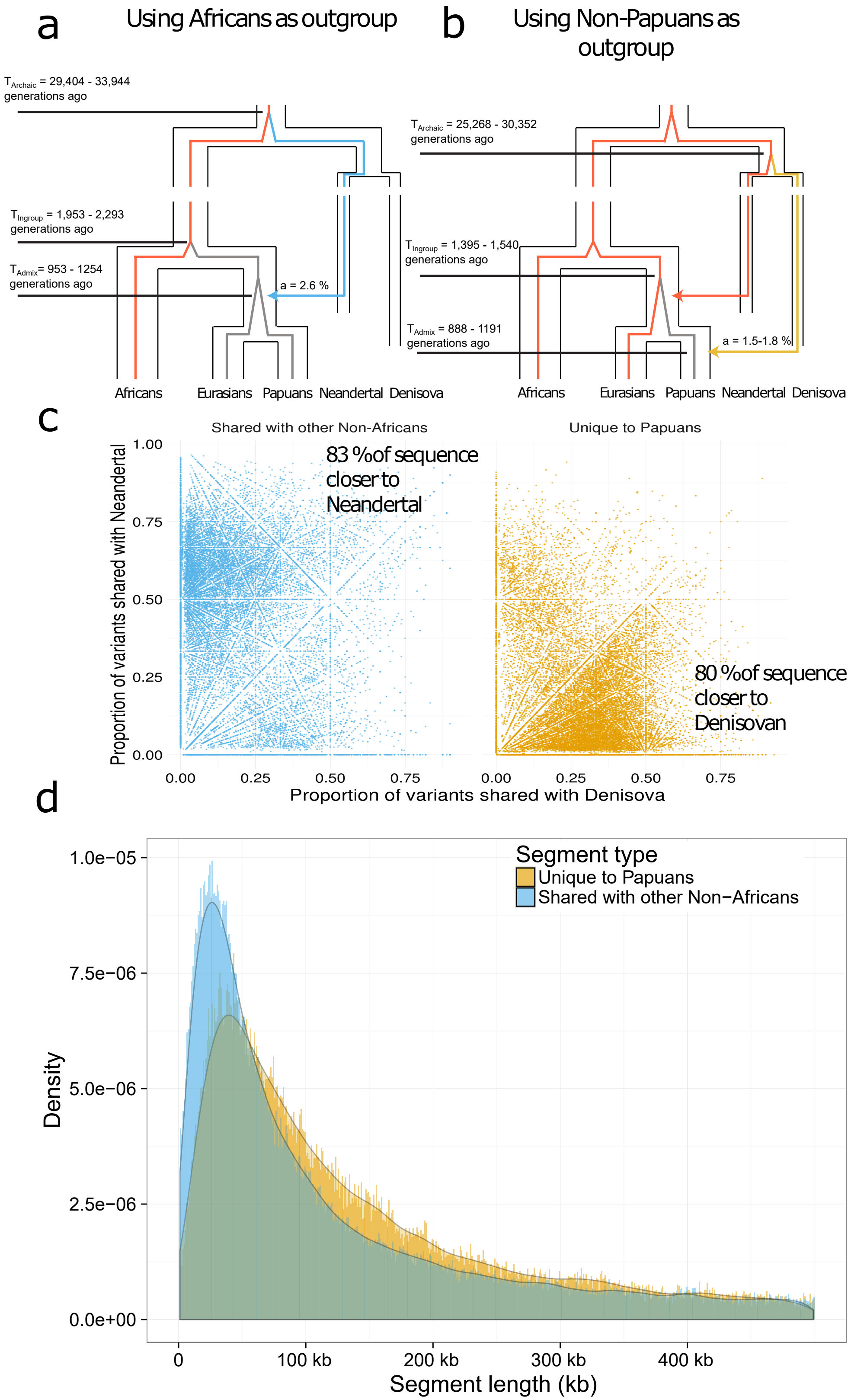
a
Using Africans as outgroup
b
Using Non-Papuans as outgroup
T Archaic = 29,404 - 33,944 generations ago
T Ingroup = 1,953 - 2,293 generations ago
T Admix= 953 - 1254 generations ago
a = 2.6 %
Africans
Eurasians
Papuans
Neandertal
Denisova
T Archaic = 25,268 - 30,352 generations ago
T Ingroup = 1,395 - 1,540 generations ago
T Admix = 888 - 1191 generations ago
a = 1.5-1.8 %
Africans
Eurasians
Papuans
Neandertal
Denisova
c
Shared with other Non-Africans
Unique to Papuans
83 %of sequence closer to Neandertal
80 %of sequence closer to Denisovan
Proportion of variants shared with Neandertal
Proportion of variants shared with Denisova
0.00
0.25
0.50
0.75
1.00
d
Segment type
Unique to Papuans
Shared with other Non−Africans
Density
1.0e−05
7.5e−06
5.0e−06
2.5e−06
0.0e+00
0
100 kb
200 kb
300 kb
400 kb
Segment length (kb)